Dynamic Temperature-Aware Reliability Modeling for Multi-Branch Interconnect Trees

Jiangtao Peng*, Hai-Bao Chen*, Hengyang Zhao†, Zeyu Sun†, and Sheldon X.-D. Tan†
* Department of Micro/Nano-electronics, Shanghai Jiao Tong University, Shanghai 200240, China
† Department of Electrical and Computer Engineering, University of California, Riverside, CA 92521, USA

Abstract—**In high performance circuit design, thermal effect on electromigration (EM) reliability has become a recent major research for being a limiting factor. In this paper, we propose a novel analytic method to calculate the stress evolution considering time-varying temperature effects during the void nucleation phase for multi-branch interconnect trees, including the straight-line three-terminal wires, the T-shaped four-terminal wires and the cross-shaped five-terminal wires. The proposed closed-form expression can be used to calculate the hydrostatic stress evolution with time-varying temperature. Experiment results show that the obtained analytic solutions match well with the numerical results calculated using COMSOL and thus the proposed models can be used in traditional EM reliability analysis tools.**

I. INTRODUCTION

Electromigration in circuit and system level design has recently been an important reliability issue which is related to several important aspects such as current density, temperature, micro/nano structures, and properties of materials and devices [1]–[3]. Traditionally electromigration reliability has been guaranteed on design for manufacturing by providing current-limiting design rules. However, reliance on current density alone does not provide an accurate assessment of electromigration induced failure, since thermal migration induced by temperature gradient and stress migration induced by thermo-mechanical stress also influence the formation of damage [4] [5] [6].

Current design rules developed to prevent EM-based failure tend to be more conservative than considering the factors affecting electromigration such as temperature change and metal wire structure [3]. The diffusion rate of metal atoms is affected by the temperature because the diffusivity of atoms depends exponentially on the temperature. Existing EM models mainly focused on the very-large-scale integration (VLSI) failure analysis at a constant temperature and they did not reveal the reliability impacts caused by time-varying temperature [7]. Recently, some EM models have been proposed to avoid the drawbacks of using a constant temperature during electromigration [8]. However, these EM models still estimate the lifetime of each time interval with a constant temperature based on the Korhonen's equation.

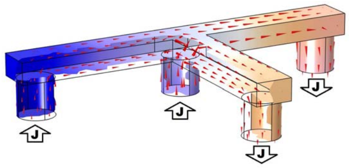

Fig. 1. Electrical current in a 3-terminal wire structure (J: current direction)

Modeling, simulation, and experimental analysis of interconnect reliability have primarily focused on simple straight-line interconnects [9]. In order to solve this problem, more compact physics-based EM models were proposed recently [10] [11] for a few important metal interconnection structures such as the one shown in Fig. 1. However, those analytical expressions still cannot provide the EM-induced hydrostatic stress evolution with time-varying ambient temperature, which ultimately determines the VLSI failures. In view of this, the purpose of this paper is for the first time to calculate the stress evolution considering time-varying temperature effects during the void nucleation phase for some multi-branch interconnect trees, including the straight-line there-terminal wires, the T-shaped four-terminal wires and the cross-shaped five-terminal wires.

II. TEMPERATURE EFFECT ON ELECTROMIGRATION

Stress evolution due to electromigration in interconnect lines is an important concern in estimating VLSI failures. In 1993, Korhonen [9] proposed physically based analytical model for mechanical stress evolution during electromigration in a confined metal line described by a one-dimensional equation, given by

$$\frac{\partial \sigma(x,t)}{\partial t} = \frac{\partial}{\partial x}\left[D_t\left(\frac{\partial \sigma(x,t)}{\partial x} + G\right)\right] \tag{1}$$

where σ is the hydrostatic stress, $D_t = \frac{D_r B \Omega}{kT(t)}$ is the stress diffusivity affected by the temperature $T(t)$ and $G = \frac{Z^* e \rho}{\Omega} j$ is the EM driving force. Here, D_r is the atomic diffusivity, B is the effective bulk modulus, Ω is the atomic volume, k is the Boltzman's constant, Z^* is the effective charge number, e is the electron charge, ρ is the resistivity, t is time, and j is current density. Moreover, $D_r = D_0 e^{-\frac{E_0}{kT(t)}}$ is the effective atomic diffusion coefficient, and D_0 and E_0 stand for the pre-exponential factor and the activation energy, respectively.

This work is supported in part by the Nature Science Foundation of China (NSFC) under No. 61604095, in part by a 985 research fund from Shanghai Jiao Tong University, and in part by NSF Grant under No. CCF-1527324. *Correspondence author: Hai-Bao Chen. Email: haibaochen@sjtu.edu.cn.*

978-1-5090-6625-4/17/$31.00 ©2017 IEEE

It should be noted that the temperature $T(t)$ changes over the time t in real circuits. In the following sections, the temperature over time is assumed to be modeled with a sine/square wave as shown in Fig. 2(a).

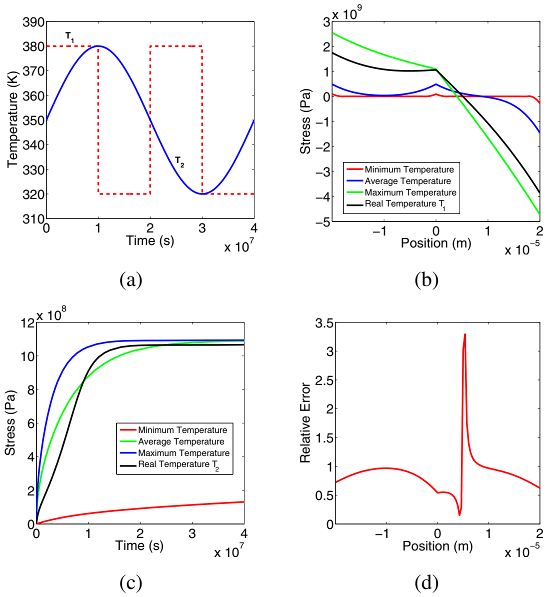

(a) (b)

(c) (d)

Fig. 2. (a) Temperature profiles over time used for simulation: square wave (T_1) and sine wave (T_2). (b) The EM stress developments along one simple straight-line three-terminal wire. (c) The EM stress development at the center of this simple wire. (d) The relative error between the average and actual temperature profiles for stress simulation.

To observe the effects of varying temperature on EM analysis, the square (T_1) and sine (T_2) waves are used to model the changes in temperature over a period of time which can be seen from Fig. 2(a). The EM stress developments along one simple straight-line wire under minimal/average/maximum/real temperature profiles are shown in Fig. 2(b) from which we can see that there are big differences between these simulation results. Fig. 2(c) shows the EM stress developments over time at the center of this simple wire under different temperature profiles. Besides, it can also be seen from Fig. 2(d) that the relative error between the stress values under the actual and average temperatures is mostly greater than 50%. Thus, we need to develop an exact dynamic stress model for the VLSI interconnect tree for prediction of interconnect lifetime for any time-dependent temperature profile.

III. DYNAMIC TEMPERATURE-AWARE MODELING FOR EM RELIABILITY ANALYSIS

A. *Unified stress evolution equation*

In this section, we establish a unified equation for describing the stress evolution process during the void nucleation for multi-branch interconnect trees shown in Fig.3. The simple single segments in these trees are connected through the center node "0". Without loss of generality, we assume that the interconnect tree has m segments which have the same length L. In order to derive a unified equation describing the stress evolution for each segment, the rectangular coordinate system centered at the node "0" can be used for indicating the location of each branch. Thus, a unified equation describing stress evolution during the void nucleation phase for these multi-branch interconnect trees can be established as follows

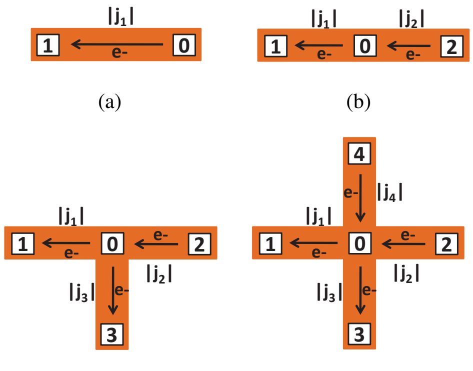

(a) (b)

(c) (d)

Fig. 3. The direction of the current is indicated by the arrow: (a) single line wire ("I" shape); (b) three-terminal wire ("dotted I" shape); (c) four-terminal wire ("T" shape); (d) cross-shaped five-terminal wire ("+" shape).

$$\begin{aligned}\frac{\partial\sigma_{2a+1}(x,t)}{\partial t} &= \frac{\partial}{\partial x}[D_{t,2a+1}(\frac{\partial\sigma_{2a+1}(x,t)}{\partial x}+G_{2a+1})]\\ &\qquad \texttt{in } -L<x<0,\ t>0,\\ \frac{\partial\sigma_{2b+2}(x,t)}{\partial t} &= \frac{\partial}{\partial x}[D_{t,2b+2}(\frac{\partial\sigma_{2b+2}(x,t)}{\partial x}+G_{2b+2})]\\ &\qquad \texttt{in } 0<x<L,\ t>0,\end{aligned} \tag{2}$$

where $a=0,1,\cdots,\lfloor(m-1)/2\rfloor$ and $b=0,1,\cdots,\lfloor m/2\rfloor-1$. It should be noted that the atom flux and the stress value must be continuous at the joint point "0", which can be reflected by the following boundary conditions

$$\begin{aligned}&D_{t,2a+1}(\frac{\partial\sigma_{2a+1}(x,t)}{\partial x}+G_{2a+1})=0, \texttt{at } x=-L,\ t>0,\\ &D_{t,2b+2}(\frac{\partial\sigma_{2b+2}(x,t)}{\partial x}+G_{2b+2})=0, \texttt{at } x=L,\ t>0,\\ &\sigma_{2a+1}(x,t)=\sigma_{2b+2}(x,t),\ \texttt{at } x=0,\ t>0\\ &\sum_{a=0}^{\lfloor(m-1)/2\rfloor} D_{t,2a+1}(\frac{\partial\sigma_{2a+1}(x,t)}{\partial x}+G_{2a+1}),\\ &=\sum_{b=0}^{\lfloor m/2\rfloor-1} D_{t,2b+2}(\frac{\partial\sigma_{2b+2}(x,t)}{\partial x}+G_{2b+2}),\ x=0,\ t>0.\end{aligned} \tag{3}$$

We assume that there is no stress anywhere in the whole tree at the initial time $t=0$. For the sake of simplicity, we also assume that each branch has the same diffusivity, i.e., $D_{t1}=D_{t2}=\cdots=D$ and $\beta_1=\beta_2=\cdots=\beta=\sqrt{\frac{s}{D}}$. In order to obtain the analytical solution $\sigma_i(x,t)$ by using the Laplace transform technique, we need to introduce the following notations

$$\begin{aligned}&\xi_0(x,q)=4qL-x, && \eta_0(x,q)=4qL+x,\\ &\xi_1(x,q)=(1+4q)L-x, && \eta_1(x,q)=(1+4q)L+x,\\ &\xi_2(x,q)=(2+4q)L-x, && \eta_2(x,q)=(2+4q)L+x,\\ &\xi_3(x,q)=(3+4q)L-x, && \eta_3(x,q)=(3+4q)L+x,\\ &\xi_4(x,q)=(4+4q)L-x, && \eta_4(x,q)=(4+4q)L+x,\end{aligned} \tag{4}$$

where n is a nonnegative integer. Also, we need to construct the following basic function

$$g(x,t) = 2\sqrt{\frac{\kappa t}{\pi}} e^{-\frac{x^2}{4\kappa t}} - x \times \texttt{erfc}\{\frac{x}{2\sqrt{\kappa t}}\}. \tag{5}$$

where $\texttt{erfc}\{x\} = \frac{2}{\sqrt{\pi}} \int_x^{+\infty} e^{-t^2} dt$ is the complementary error function. We omit the details here due to space limit. Using the notations mentioned above, we can get the exact analytical solution of the stress evolution equation for each segment:

$$\begin{aligned} \sigma_{2a+1} = & \frac{1}{m} \sum_{q=0}^{+\infty} \{2(G_{sum} - G_{2a+1}) g(\xi_1, t) + m G_{2a+1} g(\xi_3, t) \\ & - (m-2) G_{2a+1} g(\xi_1, t) - G_{sum}(g(\xi_0, t) + g(\xi_2, t))\} \\ & + \frac{1}{m} \sum_{q=0}^{+\infty} \{2(G_{sum} - G_{2a+1}) g(\eta_3, t) + m G_{2a+1} g(\eta_1, t) \\ & - (m-2) G_{2a+1} g(\eta_3, t) - G_{sum}(g(\eta_2, t) + g(\eta_4, t))\}, \end{aligned} \tag{6}$$

$$\begin{aligned} \sigma_{2b+2} = & \frac{1}{m} \sum_{q=0}^{+\infty} \{2(G_{sum} + G_{2b+2}) g(\xi_3, t) - m G_{2b+2} g(\xi_1, t) \\ & + (m-2) G_{2b+2} g(\xi_3, t) - G_{sum}(g(\xi_2, t) + g(\xi_4, t))\} \\ & + \frac{1}{m} \sum_{q=0}^{+\infty} \{2(G_{sum} + G_{2b+2}) g(\eta_1, t) - m G_{2b+2} g(\eta_3, t) \\ & + (m-2) G_{2b+2} g(\eta_1, t) - G_{sum}(g(\eta_0, t) + g(\eta_2, t))\}, \end{aligned} \tag{7}$$

where $G_{sum} = \sum_{a=0}^{\lfloor (m-1)/2 \rfloor} G_{2a+1} - \sum_{b=0}^{\lfloor m/2 \rfloor - 1} G_{2b+2}$. It should be noted that the dominant one-term approximation can achieve sufficient accuracy for practical EM analysis, which will be addressed later in experimental section.

B. Dynamic EM-induced stress modeling

We start with the EM-induced stress evolution equation as shown in (2) and assume that the current density does not change over time, namely, the term $G = \frac{Z^* e \rho}{\Omega} j$ is constant. Under the assumption of time-dependent temperature, the stress diffusivity D_t is a function of time.

For deriving the proposed dynamic EM model, we need to rewrite the stress evolution $\sigma(x,t)$ as $\sigma(x,t,D_t)$. Also, we assume that $D_t(T(t))$ can be partitioned into j small segments:

$$D_t(T(t)) = \begin{cases} D_1, 0 \le t \le \Delta t_1 \\ D_2, \Delta t_1 < t \le \Delta t_1 + \Delta t_2 \\ \cdots, \\ D_l, \sum\limits_{i=1}^{l-1} \Delta t_i < t \le \sum\limits_{i=1}^{l} \Delta t_i \quad l = 2, 3, \cdots, \end{cases} \tag{8}$$

where D_l is the average value over the time interval $(\sum\limits_{i=1}^{l-1} \Delta t_i, \sum\limits_{i=1}^{l} \Delta t_i]$. If the interval size is small enough, D_l can stand for the value of diffusivity at a specific time t. Considering the same initial and conditions for the stress evolution equation (1), let $\sigma(x,t,D_1)$ and $\sigma(x,t,D_2)$ be the solutions to the equation with $D_t = D_1$ and $D_t = D_2$, respectively. Assuming that $\sigma(x,t,D_1)$ is a known solution, we obtain $\frac{\partial \sigma(x,t,D_1)}{\partial t} = \frac{\partial}{\partial x}[D_1(\frac{\partial \sigma(x,t,D_1)}{\partial x} + G)]$. We note that $\frac{\partial \sigma(x,t,D_2)}{\partial t} = \frac{D_2}{D_1} \frac{\partial \sigma(x,\frac{D_2}{D_1}t,D_1)}{\partial t}$ and $\frac{\partial \sigma(x,t,D_2)}{\partial x} = \frac{\partial \sigma(x,\frac{D_2}{D_1}t,D_1)}{\partial x}$, which leads to $\frac{\partial \sigma(x,t,D_2)}{\partial t} = \frac{\partial}{\partial x}[D_2(\frac{\partial \sigma(x,t,D_2)}{\partial x} + G)]$. Thus, $\sigma(x,t,D_2) = \sigma(x, \frac{D_2}{D_1}t, D_1)$ is the solution to the stress equation (1) with $D = D_2$.

The stress build-up process for time-varying temperature in multi-branch interconnect trees can be independent of the value of $T(t)$ in (6) and (7). By derivation the stress over a period time Δt_1 with the temperature value T_1 will be equal to the stress over a period time $\frac{D_t(T_2)}{D_t(T_1)} \Delta t_1$ with the temperature T_2. Thus, the expressions (6) and (7) under constant temperature can be used to describe the stress evolution under time-varying thermal condition. At any given time $t = \sum\limits_{i=1}^{l-1} \Delta t_i$, a dynamic EM model for multi-branch interconnect trees can be used to calculate the stress evolution $\sigma_{p,th}(x,t,D)$ with time-varying temperature profile, given by

$$\sigma_{p,th}(x, \sum_{i=1}^{l-1} \Delta t_i, D_t) = \sigma_p(x, \sum_{i=1}^{l-1} \frac{D_i}{D_1} \Delta t_i, D_1) \tag{9}$$

where $\sigma_p(x,t,D)$ $(p = 1, 2, \cdots)$ is given by (6) and (7).

IV. EXPERIMENTAL RESULTS AND DISCUSSIONS

The proposed dynamic EM model considering time-varying temperature effect for multi-branch interconnect trees have been implemented in Matlab and compared with the finite element analysis tool COMSOL [12]. In the simulations to be described below, the following parameter values are used: $Z^* = 10$, $\rho = 3 \times 10^{-8} \Omega/m$, $\Omega = 8.78 \times 10^{-30} m^3$, $B = 5.5 \times 10^{10} Pa$, $D_0 = 5.5 \times 10^{-5} m^2/s$, $E_0 = 1.1 eV$, $e = 1.6 \times 10^{-19} C$, $k = 1.38 \times 10^{-23} J/K$. The length of each segment is set to be $L = 2 \times 10^{-5} m$.

We first analyze the three-terminal interconnect tree with two segments with the current flow directions as shown in Fig.3(a). Fig.4 shows the stress evolution and distribution for this interconnect tree. It can be seen from Fig.4(a) and Fig.4(b) that the analytical solution obtained by the proposed method fits well to the numerical simulation results obtained by COMSOL at every time instance. Fig.4(c) and Fig.4(d) show the stress evolutions at a fixed location in the interconnect tree under the square-wave and sine-wave temperature profiles, respectively. In the case of the dynamic stress evolution by using square-ware temperature profile, it can be seen from Fig.4(c) that the stress value at the cathode changes dramatically when the temperature varies from $380K$ to $320K$ or from $320K$ to $380K$. For both the cases of square-wave and sine-wave temperatures, the proposed dynamic model can match well with the simulation results obtained from COMSOL. We can see from Fig.4(c) and Fig.4(d) that a great difference will be caused by using an average temperature instead of the actual temperature profile.

For the T-shaped four-terminal interconnect tree shown in Fig. 3(c), the current densities in each segment are set to be $j_1 = 2 \times 10^{10} A/m^2$, $j_2 = 4 \times 10^{10} A/m^2$, $j_3 = 6 \times 10^{10} A/m^2$, respectively. The stress evolution along the segments “10” and “02” is shown in Fig. 5(a) for square-wave environment, and Fig. 5(b) shows the stress evolution under this time-varying temperature profile. It can be seen from Fig. 5(b)

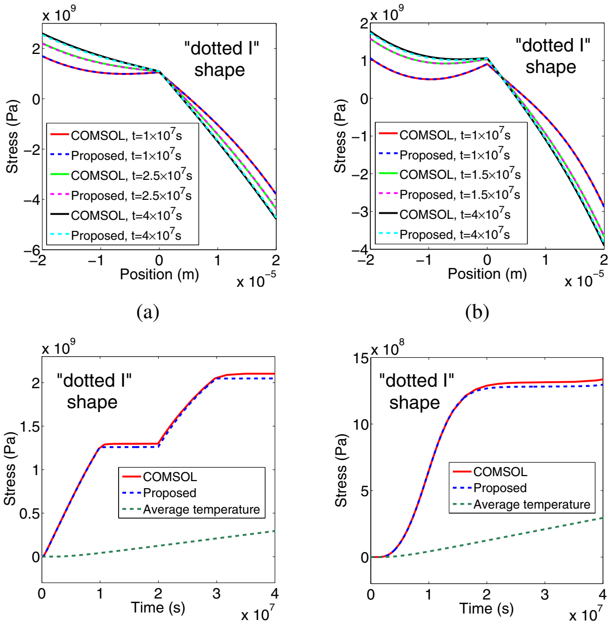

(a) (b)

(c) (d)

Fig. 4. Simulation results for the three-terminal straight-line interconnect tree: $j_1 = 2 \times 10^{10} A/m^2$, $j_2 = 6 \times 10^{10} A/m^2$. (a) Stress evolution considering the square-wave temperature. (b) Stress evolution under the sine-wave temperature profile. (c) Stress evolution over time at the cathode considering the square-wave temperature. (d) Stress evolution over time at the cathode under the sine-wave temperature profile.

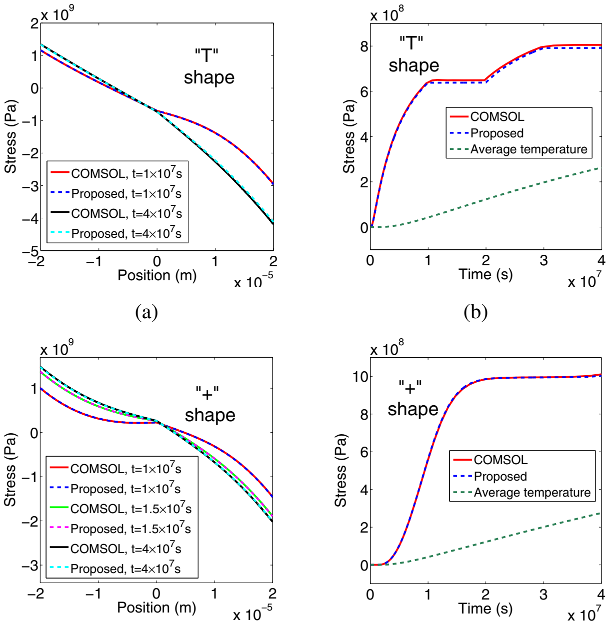

(a) (b)

(c) (d)

Fig. 5. The "T"-shape interconnect tree under the square-wave temperature profile: (a) stress evolution along the segments "10" and "02",(b) stress evolution over time at the cathode; the "+"-shape interconnect tree considering the sine-wave temperature: (c) stress evolution along the segments "10" and "02"; (d) stress evolution over time at the cathode.

that an obvious error will occur due to the usage of the average temperature for the EM-induced lifetime calculation. For further simulation and analysis, the current densities in the the cross-shaped five-terminal interconnect tree are assumed to be $j_1 = 2 \times 10^{10} A/m^2$, $j_2 = 3 \times 10^{10} A/m^2$, $j_3 = 4 \times 10^{10} A/m^2$, and $j_4 = 5 \times 10^{10} A/m^2$. Again, we can see from Fig. 5(c) and Fig. 5(d) that the analytical model fits well the COMSOL simulation results and using the average temperature for calculation of stress evolution may result in large errors for VLSI circuit lifetime estimation.

V. CONCLUSION

In this paper, we have proposed a dynamic modeling and analysis method for EM reliability analysis in multi-branch interconnect trees, including the straight-line three-terminal wires, the T-shaped four-terminal wires and the cross-shaped five-terminal wires, which reflects practical VLSI interconnect architectures and interconnect layout-design techniques. The obtained closed-form expression can be used to calculate the EM-induced stress evolution under under time-varying temperature environment. The numerical comparison results show that the proposed analytical solution matches well with the finite element analysis obtained from COMSOL.

REFERENCES

[1] D.-A. Li, M. Marek-Sadowska, and S. R. Nassif, "A method for improving power grid resilience to electromigration-caused via failures," *IEEE Transactions on Very Large Scale Integration Systems*, vol. 23, no. 1, pp. 118–130, 2015.

[2] H.-B. Chen, S. X.-D. Tan, V. Sukharev, X. Huang, and T. Kim, "Interconnect reliability modeling and analysis for multi-branch interconnect trees," in *Design Automation Conference*, pp. 1–6, 2015.

[3] R. Kanapady, D. Moore, A. Raghupathy, and W. Maltz, "Influence of temperature gradient on electromigration failures in 3D packaging," in *Intersociety Conference on Thermal and Thermomechanical Phenomena in Electronic Systems*, pp. 70–76, 2016.

[4] M. Li, K. N. Tu, D.-W. Kim, and S. Gu, "Electromigration induced thermomigration in microbumps by thermal cross-talk across neighboring chips in 2.5D IC," in *IEEE International Reliability Physics Symposium*, pp. PA–3–1–PA–3–4, 2016.

[5] H. V. Nguyen, C. Salm, B. Krabbenborg, K. Weide-Zaage, J. Bisschop, A. J. Mouthaan, and F. G. Kuper, "Effect of thermal gradients on the electromigration lifetime in power electronics," in *IEEE International Reliability Physics Symposium*, pp. 619–620, 2004.

[6] H.-B. Qin, W. Yue, X.-P. Zhang, and D.-G. Yang, "Size and geometry effects on the electromigration behavior of flip-chip Sn3.5Ag solder joints," in *International Conference on Electronic Packaging Technology*, pp. 651–655, 2015.

[7] K. Nikawa, K. Nasu, M. Murase, T. Kaito, T. Adachi, and S. Inoue, "New applications of focused ion beam technique to failure analysis and process monitoring of VLSI," in *IEEE International Reliability Physics Symposium*, pp. 43–52, 1989.

[8] Z. Lu, W. Huang, J. Lach, M. Stan, and K. Skadron, "Interconnect lifetime prediction under dynamic stress for reliability-aware design," in *IEEE/ACM International Conference on Computer Aided Design*, pp. 327–334, 2004.

[9] M. A. Korhonen, P. Børgesen, K. N. Tu, and C.-Y. Li, "Stress evolution due to electromigration in confined metal lines," *Journal of Applied Physics*, vol. 73, no. 8, pp. 3790–3799, 1993.

[10] X. Huang, T. Yu, V. Sukharev, and S. X.-D. Tan, "Physics-based electromigration assessment for power grid networks," in *Design Automation Conference*, pp. 1–6, 2014.

[11] V. Sukharev, "Beyond blacks equation: Full-chip EM/SM assessment in 3D IC stack," *Microelectronic Engineering*, vol. 120, pp. 99–105, 2014.

[12] "Comsol mutiphysics: User guide." www.comsol.com.